Semiclassical interatomic potential for carbon and its application to the self-interstitial in graphite

1991 J. Phys.: Condens. Matter 3 3065

(http://iopscience.iop.org/0953-8984/3/18/002)

J. Phys.: Condens. Matter 3 (1991) 3065–3079. Printed in the UK

Semiclassical interatomic potential for carbon and its application to the self-interstitial in graphite

Malcolm I Heggie†

Department of Physics, Stocker Road, University of Exeter, Exeter EX4 4QL, UK

Received 19 December 1990

Abstract. A semiclassical interatomic potential for carbon is discussed which is based on the proximity cell (the Wigner–Seitz cell) around each atom. It introduces three internal degrees of freedom per atom, representing the magnitude and direction of the p orbital that is not involved in sp hybridization. Its direct interpolation between sp^2 and sp^3 configurations combined with good elastic properties allows its use on problematic defects, such as the interplanar interstitial in graphite, which is given as an example.

1. Introduction

Carbon in its many forms has a wealth of technological applications, from carbon fibres to diamond-like films, from graphite moderators to chemical filters and catalysts. Its two most important, and almost energetically degenerate, allotropes are graphite and diamond, which exhibit wildly disparate properties, mechanical ones in particular. In order to model these properties and how they combine in non-crystalline solids of intermediate structure we propose a semiclassical potential which has two aims. First, to include the essential quantum mechanical behaviour of electrons in atoms and bonds, already understood as 'chemical intuition', and, second, to maximize the input from existing experimental and theoretical energetics data. In a sense the potential is a crude expert system, with chemical rules forming the framework used to elicit and reproduce numerical detail from experimental and *ab initio* information.

One important consideration that will distinguish it from recent classical interatomic potentials is the reproduction of all the experimental elastic constants for the diamond and graphite structures, allowing correct long-range relaxation behaviour around defects.

The aim of this paper is to put the concept of the potential in context and to describe how it is reduced to practice. Finally an application, namely that of the interplanar interstitial in graphite, is discussed which illustrates all the properties of the potential.

† Present address: Department of Computer Science, Prince of Wales Road, University of Exeter, Exeter EX4 4PT, UK.

0953-8984/91/183065+15$03.50

2. The context

The classical-potential approach to computing the energetics of solids has the instant appeal of computational efficiency. Historically many potentials have started from the premiss that electron kinetic energy terms in the Hamiltonian decide the ionic and/or bond charges only at the outset of the calculation. Typical of this approach is the rigid-ion model with formal charges, where electronic kinetic energy causes one element's highest occupied orbital to be substantially higher in energy than the lowest unfilled orbital of another element. Transfer of an integral number of electrons from atoms of one element to those of the other element can give rise to a compound whose binding is dominated by electrostatic interactions. Even when the possibility of fitted partial charges is allowed, the common assumption is that kinetic energy stays constant while the electrostatic energy of some idealized charge distribution is minimized. Two concessions to kinetic energy exist:

(i) in ionic models the ion cores are held to repel each other by a central force that is said to originate in the overlap of ion-core wavefunctions with those on neighbouring sites and

(ii) in valence force models (and three body additions to ionic models) the tendency of an sp^3 hybridized atom to prefer a tetrahedral environment is simulated by an expansion of the energy, frequently in bond angle and length, around the perfect tetrahedral energy minimum.

In the latter case the expansions must always have limited validity away from the perfect environment, but they have been extremely useful in the analysis and understanding of phonon and infrared spectra of semiconductors and in the examination of conformational properties of molecules. Similarly, ionic models continue to enjoy conspicuous success for the same properties of minerals. Unfortunately, the approximations involved in ionic and valence force potentials inhibit their use in the study of defects, not least because of ambiguities in the definition of bonds in a defect.

Given the fact that the problem involves an optimization of total electronic and nuclear energy, and that, in defects at least, neither electrostatic energy nor electronic kinetic energy dominate, it would appear natural to compute everything from first principles. This is currently impractical for many physically realistic systems, but there has been pronounced success in the application of local density functional theory and norm-conserving pseudopotentials to small clusters and supercells (e.g. Yin and Cohen 1984, Srivastava and Weaire 1987, Pandey 1986, Biswas *et al* 1984, Heggie *et al* 1991). For the larger systems necessary in most materials science problems, a more efficient method is required and a common approximation is to parametrize a model tight-binding Hamiltonian and use this to give structural properties, notably of grain boundaries (Paxton and Sutton 1989) and surfaces (Chadi 1984). The idea is to compute the Hamiltonian matrix in a basis of atomic-like orbitals and to diagonalize it either as a whole, directly, or locally by recursion and moments. Most often, orthogonal atom-centred orbitals are assumed, but since the overlap interaction between neighbouring orbitals is responsible for the repulsion that resists collapse of the crystal (Harrison 1986), the effect of overlap is added later as a central interatomic force. The total energy is taken as a sum over the occupied one-electron eigenvalues or, if the local densities of states are calculated, a sum over atoms of the integral of the first moment of the local density of states. Some tight-binding prescriptions keep all atoms neutral while others allow charge transfer. Unfortunately, taking the energy from a sum of

one-electron eigenvalues double-counts the ion–electron and electron–electron electrostatic interactions, so it is implied that the term that corrects for double counting is included in the central-force repulsion. Thus the parametrized tight-binding method is firmly rooted in quantum mechanics and, since electron occupation is decided by linear combinations of basis orbitals, it is possible to optimize the energy, at least with respect to electron occupation, very efficiently.

The desirable properties of the method, such as automatic accounting for valency via electron occupation and giving guidance on electronic energy levels in defects, are counterbalanced by several questions of consistency. First of all, the assumed orthogonal atomic-like orbitals would be long ranged, whereas non-zero Hamiltonian matrix elements are normally only assigned to nearest neighbours. Second, there is no justification for assuming that either the ion–ion repulsion or the double-counting correction should be a central force. Third, good parameters for structural properties do not give good band structures and the appropriate scaling of parameters with distance is not universally agreed. Fourth, charge self-consistency and large basis sets are both known to be extremely important in *ab initio* total energy calculations, yet these are substantially denied in tight binding, where the basis is charge independent and minimal. These problems cast doubt on the wisdom of parametrizing at the electron Hamiltonian matrix element level and suggest that the complex implications of the electronic Hamiltonian might be better simulated by a clever function of atomic coordinates.

In recent developments of classical potentials researchers have tried to simulate a wide range of covalent and metallic systems using functions of bond lengths and angles (e.g. Stillinger and Weber 1985, Tersoff 1986, 1988a, b) or more general two- and three-body terms (e.g. Biswas and Hamann 1985). In other words, they have tried to include implicitly the variation in electronic kinetic energy between structures. These have had a degree of success, although typically they either suffer from too limited a base for parametrization (Stillinger–Weber) or too limiting a potential form (Biswas–Hamann). However, Tersoff's potential appears to have had at least as much success as many and the potential proposed here develops the ideas in Tersoff's potential to achieve a more accurate description of a wider range of covalent structures. The Tersoff potential has also been shown to be equivalent to the embedded atom method (Brenner 1989), which is very successful in metals, and the embedded atom method has been applied to graphite using a Buckingham interlayer potential (Oh and Johnson 1989).

In this work two drawbacks to the Tersoff potential will be removed: first, the arbitrary radial cut-off for interactions and, second, the opaque nature of the bond length–bond angle formula that expresses 'competition' between bonds. However, the systematic framework we shall introduce also has drawbacks—it is relatively more computationally intense and it is not analytical, invoking three internal degrees of freedom per atom (corresponding to the magnitude and direction of an unhybridized p orbital).

3. The potential

The potential starts from the premiss that the best rotationally-invariant description of the local environment of an atom is the Wigner–Seitz or proximity cell. Different cells are characteristic of different structures; the single proximity cell of the diamond structure is illustrated in figure 1 and the two distinct cells of hexagonal graphite in

figure 2. Notice that in essence the diamond structure gives a tetrahedron, while the graphite a triangular prism. Second neighbours in the diamond structure and stacking relationships in the graphite structure lead to corner truncation.

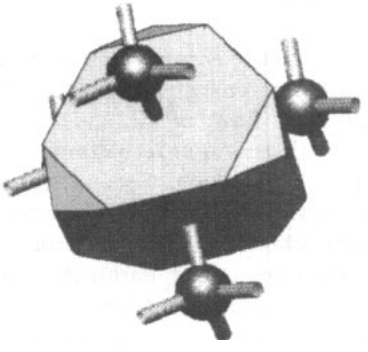

Figure 1. Proximity cell of diamond.

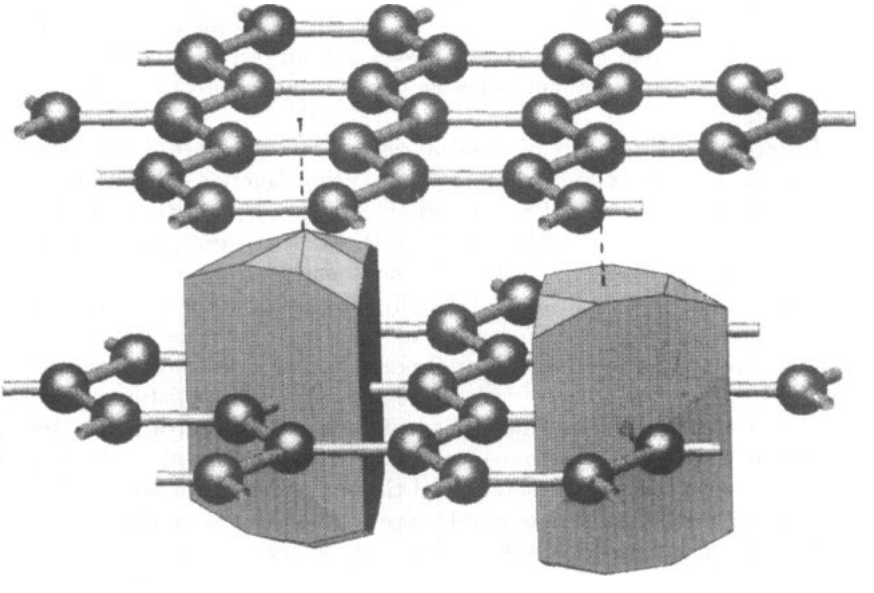

Figure 2. Proximity cells of graphite.

The philosophy behind the potential allows that the most important interactions are those between atoms that share proximity cell faces. Furthermore the face shared between two atoms must contain the intercept with their internuclear vector in order for the interaction to be non-negligible. Part of the physical reasoning behind the potential is that every point within the proximity cell of atom i is closer to i than to any other atom and a bond must be weak if one atom cannot 'see' another because the electron density on intervening atoms should have sufficient freedom to screen out their interactions. Thus, in addition to r_{ij}, the vector joining atoms i and j, a good indicator of the strength of an interaction between two atoms i and j sharing a proximity cell face is the radius of the maximum inscribed circle in the face centred on

the internuclear intercept. The bond or face parameter, $r_{\sigma_{ij}}$, is based on this radius and described in appendix A.

In order to achieve this screening approximation smoothly and consistently, interactions are modified by a function, f, of the form below:

$$f(a,a_l,a_u) = \begin{cases} 0 & a < a_l \\ \frac{1}{2}\{1-\cos[\pi(a-a_l)/(a_u-al)]\} & a_l < a < a_u \\ 1 & a_u < a \end{cases}$$

where, for example, the variable a will often be a function of $r_{\sigma_{ij}}$ such as $a = 2r_{\sigma_{ij}}/r_{ij}$. The function goes smoothly to zero with no gradient at $r_{\sigma_{ij}} = 0$ when $a_l > 0$ and it saturates at unity for $a > a_u$, when the structure is close to perfect graphite or perfect diamond. This flatness for $a > a_u$ allows the behaviour around the graphite and diamond structure energy minima to be 'fine tuned' by smaller terms, such as V_K described later. The parameters a_l and a_u determine the position and steepness of the cut-off.

The potential has been devised to interpolate between diamond and graphite structures and does this with functions, h, that depend on a parameter ϕ linearly, with $\phi = 0$ corresponding to diamond and $\phi = 1$ corresponding to graphite. Any variable which has ϕ as a parameter in the following equations is understood to be such a linear interpolation with the values at $\phi = 0$ and $\phi = 1$ fitted, respectively, to diamond and graphite data.

$$h(\phi) = (1-\phi)h(0) + \phi h(1)$$

The first proximity cell potential for silicon (Heggie 1989) did not invoke any internal degrees of freedom for atoms and was single valued. This is the best state of affairs for an efficient potential. Unfortunately, for graphite it has been found necessary to include the magnitude and direction of the unhybridized p orbital, $\mathbf{p}_i$ on atom i, $|\mathbf{p}_i|$ being between 0 (sp^3 hybridization, e.g. diamond) and 1 (sp^2 hybridization, e.g. graphite). The $\mathbf{p}_i$ are used to place extra constraints on bonding, beyond the purely geometrical ones describing the cell faces. For instance, the interaction between two atoms, i and j, connected by vector $\mathbf{r}_{ij} = \mathbf{r}_j - \mathbf{r}_i$, will be either a π bond or a σ bond depending on the vectors $\mathbf{p}'_{ij}$ and $\mathbf{p}''_{ij}$ representing the projection of $\mathbf{p}_i$ onto the bond face and $\mathbf{p}_j$ onto the latter direction, respectively, as below.

$$\mathbf{p}'_{ij} = \mathbf{p}_i - (\mathbf{p}_i \cdot \hat{\mathbf{r}}_{ij})\hat{\mathbf{r}}_{ij}$$
$$\mathbf{p}''_{ij} = (\mathbf{p}_j \cdot \hat{\mathbf{p}}'_{ij})\hat{\mathbf{p}}'_{ij}$$

There are two ways in which the $\mathbf{p}_i$ are used to generate the ϕ parameters necessary for interpolation. The first is via the atom-centred parameter $\phi_i = f(|\mathbf{p}_i|, 0, 1)$ for atom i by which the magnitude of $\mathbf{p}$ on each atom i is effectively constrained to lie between 0 and 1. This parameter controls atom-centred behaviour, such as the Keating bond bending parameters s_K, c_K and r_0 described later. The second is via the bond-centred parameter ϕ_{ij} for the bond ij:

$$\phi_{ij} = (\tfrac{1}{2}t^{-4} + \tfrac{1}{4}|\mathbf{p}'_{ij}|^{-4} + \tfrac{1}{4}|\mathbf{p}''_{ij}|^{-4})^{-\frac{1}{4}}$$
$$t = [1 - f(\Delta_{ij}, \Delta_l, \Delta_u)][\mathbf{p}_i \cdot \mathbf{p}_j |\mathbf{p}'_{ij}||\mathbf{p}''_{ij}|(2-|\mathbf{p}'_{ij}|)(2-|\mathbf{p}''_{ij}|)]^4$$

and Δ_{ij} is a combination of the two face-elongation parameters $\Delta_{1,j}$ and $\Delta_{2,j}$ described in appendix A. The combination is dominated by the smaller of the two parameters and since the smallest value of any Δ is r_σ the combination is as follows:

$$\delta_{1,j} = \Delta_{1,j} - r_{\sigma,j} \qquad \delta_{2,j} = \Delta_{2,j} - r_{\sigma,j}$$

$$\Delta_{ij} = r_{\sigma,j} + \sqrt[5]{2\delta_{1,j}^5 \delta_{2,j}^5/(\delta_{1,j}^5 + \delta_{2,j}^5)}$$

The dependence of ϕ_{ij} on Δ_{ij} simulates the geometrical limits on π bonding ; when Δ_{ij} is below Δ_l there is not enough 'space' available for a good π bond. In other words, the π bond cannot simultaneously be good and be orthogonal to the π bond in the next layer.

The terms that depend on $\mathbf{p}_i$ and $\mathbf{p}_j$ of bonded atoms i and j express the availability of these orbitals for π bonding (the condition that either has zero magnitude forces ϕ_{ij} to be zero) and the favourability of their orientation with respect to the bond face and to each other.

Both parameters ϕ_i and ϕ_{ij} are featureless in the diamond and graphite structures, giving values of 0 and 1, respectively, not only at the crystal structures but also in their vicinity. The reason for this is to allow the adjustment of elastic behaviour to be reasonably independent of the adjustment of energies of severe bonding defects that strongly affect the ϕ and the $f(2r_\sigma/r, \theta_l, \theta_u)$ terms that appear later. However, in order to fit the elastic constants there must be some interlayer coupling and some coupling between the interlayer distance and in-plane bonding; this is achieved by a modification to the ϕ_{ij} for the bonding term (which will be described later):

$$\phi' = \phi(1 - (\Delta_1 + \Delta_2 - c/2)s_1 - (\Delta_1 - c/4)^2 s_2 - (\Delta_2 - c/4)^2 s_2)$$

s_1 and s_2 being adjustable parameters, c being the graphite lattice constant and the subscript ij omitted for clarity. Note that $\Delta_1 = \Delta_2 = \frac{c}{4}$ for the three sp^2 bonds in the graphite structure.

The most significant parts of the potential comprise a Morse-like radial potential, as in the Tersoff potential (Tersoff 1986, 1988 a,b), but the radial cut-off is replaced with the many-body function $f(2r_\sigma/r, \theta_l, \theta_u)$ and the parameters of the two exponential terms are controlled by ϕ_{ij}. In total there are six parts to the potential of which V_r and V_a are the repulsive and attractive parts of the Morse-like potential, V_r^s and V_a^s are the repulsive and attractive parts of an interlayer or stacking potential for graphite, V_K is a Keating-like bond-bending potential and V_0 is an additive constant to give the reference energy.

$$V_i = \left(\sum_j (V_r)_{ij} + (V_r^s)_{ij}\right) + V_a + V_a^s + V_K + V_0$$

The formation energy, E, of a cluster is then given by $E = \Sigma V_i$.

The first two terms above are summed over all faces, ij, on the proximity cell, while V_a, V_a^s and V_K represent sums over the three or four best faces for bonding, since in the tight binding approximation only up to four independent pair bonds can be formed around an sp^3 atom.

For each face the repulsive term $(V_r)_{ij}$ is given by:

$$(V_r)_{ij} = \tfrac{1}{2}a(\phi_{ij})[1 - f(r_{ij}, r_l, r_u)]f(2r_{\sigma,j}/r_{ij}, \theta_l(\phi_{ij}), \theta_u(\phi_{ij}))\exp[-\alpha_1(\phi_{ij})r_{ij}]$$

with $a, \alpha_1, \theta_l, \theta_u$ for $\phi = 0, 1$ being adjustable constants. The role of the smooth radial cut-off is to allow the V_r potential to give way gradually to the V_r^s potential, which is adjusted for good long-range behaviour; it has very little effect because the exponent α_1 is large, making V_r small at $r = r_l$.

The stacking repulsive term V_r^s takes over gradually for $r_{ij} > r_l$ between atoms that have non-zero p components. Thus its main effect is seen in graphite, where it is largest for faces whose normals coincide with the **p** vectors on the interacting atoms i and j. These atoms are those stacked one above the other in the **c** direction.

$$(V_r^s)_{ij} = f(r_{ij}, r_l, r_u)|\mathbf{p}_i||\mathbf{p}_j|[(s_3/r_{ij}^2)f(q_{ij}, q_l, q_u) + s_3' f(q_{ij}', q_l', q_u')]$$

where

$$q_{ij} = \begin{cases} \sqrt{r_{\sigma_{ij}}}(p_{ij}''' - \frac{1}{2})^4 & p_{ij}''' > \frac{1}{2} \\ 0 & p_{ij}''' < \frac{1}{2} \end{cases}$$

$$p_{ij}''' = \sqrt{(1 - |\mathbf{p}_{ij}'|^2)(1 - |\mathbf{p}_{ij}''|^2)}$$

The constants $s_3, s_3', q_l, q_l', q_u, q_u'$ are adjustable and the first term in the square brackets dictates the perfect graphite stacking behaviour (makes graphite a local minimum with the correct elastic behaviour), while the second term ensures that graphite is a global minimum, i.e. no other stacking is lower in energy. Experimentally it is known that rhombohedral graphite (stacking ABC) is very close in energy to hexagonal graphite (only 0.18 meV per atom higher (Kelly 1981)) but in our approximation it is practically degenerate. This form of potential is similar in spirit to the recently introduced electrostatic interaction of Hunter and Sanders(1990), in the sense of having been framed with repulsive p-orbital interactions in mind.

The bonding term and the Keating term relate to the covalent bonds around each atom. The tight-binding approximation allows up to four bonds for sp^3 hybridization and three bonds for sp^2 hybridization. This potential concerns itself with interpolating between the two.

Ignoring the role of the unhybridized p orbital, the bond strength of a face representing the bond ij would be:

$$d_{ij} = \tfrac{1}{2} b(\phi_{ij}) \exp[-\alpha_2(\phi_{ij}) r_{ij}] f(2r_{\sigma_{ij}}/r_{ij}, \theta_l'(\phi_{ij}), \theta_u'(\phi_{ij}))^2$$

where $b(\phi_{ij})$ and $\alpha_2(\phi_{ij})$ are functions like $h(\phi)$ adjustable at $\phi_{ij} = 0$ and ϕ_{ij}=1. In the case of pure sp^3 bonding the covalent energy is the sum of the d_{ij} for the four faces with maximum d_{ij}. When ϕ_i is greater than zero, i.e. less than sp^3, there is the possibility of one weak bond of strength d_{ij}'' using the unhybridized p orbital and three basically sp^2 bonds of strength d_{ij}'. The latter bonds are weakened by the withdrawal of some p character.

$$d_{ij}' = d_{ij}(1 - \phi_i t'^2) \qquad d_{ij}'' = d_{ij}[1 - \phi_i(1 - t'^2)]$$

where

$$t' = 1 - f(\mathbf{p}_i \cdot \hat{\mathbf{r}}_{ij}, 0.05, 0.95)$$

Three faces/bonds A, B and C of strength d'_{ij} and one face, D, of strength d''_{ij} are chosen to maximize the covalent energy, so

$$V_a = d'_{iA} + d'_{iB} + d'_{iC} + d''_{iD}$$

The attractive interlayer potential V_a^s acts effectively between π systems in different layers, and for a given bond between atoms i and j, it is given by:

$$(V_a^s)_{ij} = \tfrac{1}{2} s_4 r_{ij} \phi_{ij} f(2r_{\sigma,ij}/r_{ij}, \theta_l(\phi_{ij}), \theta_u(\phi_{ij}))(\Delta_{1,i} + \Delta_{2,i} - c/2)$$

where $c/2$ is the graphite interlayer separation of 3.35 Å and s_4 is a free parameter. For simplicity the interaction is assumed to be linear in interlayer separation for moderate displacements. The term behaves well for moderate and large compressions, but is not suitable in this form for large expansions and surfaces. The attractive stacking potential is only effective for those interactions considered to be π bonding, i.e. A, B and C, so $V_a^s = (V_a^s)_{iA} + (V_a^s)_{iB} + (V_a^s)_{iC}$.

The term in bond angles, V_K, is of the same form as the angular part of the Keating potential (Keating 1966) but modified to take into account bond strengths, d''_{ij} and to cancel the contribution the original potential would make to the bulk modulus, which has already been fitted by the radial Morse potential. The advantage of keeping the Keating form is that it can be used alone for atoms far from a defect when dealing with defects in the diamond structure. This term only has a pronounced effect near perfect configurations, because the bond strength term d''_{ij} is modified to d^K_{ij} to reduce quickly to zero for faces that are well distorted.

$$d^K_{ij} = d'_{ij} f(2r_{\sigma_{ij}}/r_{ij}, \theta^K_l(\phi_i), \theta^K_u(\phi_i)) \qquad \text{for } j = A, B, C$$

$$d^K_{ij} = d''_{ij} f(2r_{\sigma_{ij}}/r_{ij}, \theta^K_l(\phi_i), \theta^K_u(\phi_i)) \qquad \text{for } j = D$$

$$V_K = s^K(\phi_i)\Bigg(\sum_{j=A-C} \sum_{k=j-D} d^K_{ij} d^K_{ik} [\mathbf{r}_{ij} \cdot \mathbf{r}_{ik} - r_0(\phi_i)^2 c^K(\phi_i)]^2 + \frac{1}{2} \sum_{j=A-D} d^{K^2}_{ij} (|\mathbf{r}_{ij}|^2 - r_0(\phi_i)^2)^2 c^K(\phi_i) \Bigg)$$

where c^K is a linear interpolation between the diamond and graphite values of $-\frac{1}{3}$ and $-\frac{1}{2}$, respectively, for the cosine of the equilibrium angle between bonds on the same atom in those structures.

The potential has not yet been extended to the sp hybridization case, due to lack of information about elemental structures involving triple bonds. It is easy to identify structures where sp hybridization might occur since only two, almost parallel, faces will have significant values of r_σ and d''_{ij}. The best approximation we can make is to allow that an sp σ bond cannot be worse than an sp^2 σ bond, so V_K, which would otherwise contribute strongly for angles around 180^0, is ignored on atoms for which only two or fewer bonds have $d''_{ij} > 0.6$ eV. Although this gives rise to a discontinuity in the potential, it has not affected any of the structure optimizations so far.

Table 1. Carbon parameters.

	a (eV)	b (eV)	α_1 (Å^{-1})	α_2 (Å^{-1})	θ_l	θ_u	θ_l'	θ_u'
$\phi = 0$	2948.875	78.958	4.7123	1.7006	0.0	1.4	−0.5	1.4
$\phi = 1$	2754.5	128.206	4.7123	1.9196	0.0	1.7	−1.0	1.7

	* V_0 (eV)	r_0 (Å)	s^K (Å^{-4})	c^K	θ_l^K	θ_u^K
$\phi = 0$	−7.349665	1.54049	0.0396875	$-\frac{1}{3}$	0.7	1.3
$\phi = 1$	−7.3740586	1.42028	0.0311875	$-\frac{1}{2}$	1.2	1.7

	s_1	s_2	s_3 (eVÅ^{-2})	s_3' (eV)	s_4 (eV/Å^2)	Δ_l(Å)	Δ_u(Å)
	−0.0271	0.0293	0.13	0.01	0.07	0.8	1.6

	q_l ($\sqrt{\text{Å}}$)	q_u ($\sqrt{\text{Å}}$)	q_l' ($\sqrt{\text{Å}}$)	q_u' ($\sqrt{\text{Å}}$)	r_l (Å)	r_u (Å)
	0.002633	0.05003	0.001	0.008	2.2	2.4

* Yin and Cohen 1984

4. Potential fitting

The free parameters used in the potential are given in table 1, where the reference energies are those given by the potential for diamond and graphite, being negligibly different to the cohesive energies quoted by Yin and Cohen (1984).

Because the potential is in some ways under-determined a least squares fitting was not undertaken, however the experimental elastic constants of table 2 were reproduced to within 10 % (or 3 GPa). The constants were obtained by numerical differentiation, taking account of inner elasticity using the formalism of Cousins (1982) for diamond and of an extended version for hexagonal crystals for graphite (Cousins, private communication). The internal degrees of freedom ($\mathbf{p}_i$) were frozen for the elastic constant calculation. Recently, theory and experiment have suggested that some of the graphite values may be inaccurate (Jansen and Freeman 1987, Zhao and Spain 1989) and there is nothing in the potential framework that would prevent subsequent refitting of any new accepted set of elastic constants.

Table 2. Elastic constants (GPa).

	Diamond				Graphite				
	C_{11}	C_{12}	C_{44}	ζ	C_{11}	C_{12}	C_{44}	C_{13}	C_{33}
This work	1075.1	125.4	574.1	0.21	1062.7	178.7	3.6	14.6	34.8
Experiment	1076[1]	125[1]	576[1]	0.125[1]	1060[2]	180[2]	4.0[2]	15.0[2]	36.5[2]

[1] McSkimin and Bond 1957, Cousins 1982, Cousins *et al* 1989
[2] Nicholson and Bacon 1977

Defects pose a more difficult problem, and the approach used was to choose θ_l' and θ_u', relax a chosen set of defects given in table 3, compare the model energies against

ab initio energies, re-adjust θ_l' and θ_u' and repeat the cycle until reasonable formation energies were obtained. Given the inaccuracies expected of *ab initio* calculations an exact fit was not demanded and table 3 reveals the results obtained relaxing 50 atoms around each defect. Graphite defect results were obtained with $|\mathbf{p}| = 1$ and diamond results with $|\mathbf{p}| = 0$. Squarite is a hypothetical planar carbon structure with a square 2D unit cell where every carbon atom has four in-plane neighbours. Several of the *ab initio* results, which only allowed radial relaxation around defects, should be higher in energy than those for this work where full relaxation was allowed. Thus vacancy energies and the graphite in-plane interstitial energies are more in accord with the *ab initio* results than the table indicates. Clearly, concerted exchange in diamond is the worst case.

Table 3. Defect energies (eV).

	Diamond				
	Vacancy	Bond-centred interstitial	001 split interstitial	Tetrahedral interstitial	Concerted exchange
This work	6.4	18.8	16.3	28.1	19.2
ab initio	7.2[1]	15.8[1]	16.7[1]	23.6[1]	13.2[1]

	Graphite			
	Vacancy	In-plane interstitial	Concerted exchange	Squarite (per atom)
This work	6.7	16.2	9.2	3.21
ab initio	7.6[2]	19.5[2]	10.4[2]	3.3[3]

[1] Bernholc *et al* 1988
[2] Kaxiras and Pandey 1988
[3] Weinert *et al* 1982

Finally, the region of intermediate $|\mathbf{p}|$ was explored by fitting the idealized diamond to graphite transition (diamond to rhombohedral graphite) as calculated by *ab initio* total energy methods (Fahy *et al* 1986, 1987). Table 4 shows the internal energies per atom for the transition, constraining the same parameter, R (the interlayer separation) as in the *ab initio* work, and relaxing B (the in-plane bond length) and θ (the buckling angle). The column on the right gives the magnitude of the unhybridized p orbital in the model, which moves progressively from 0 to 1 through the transition.

Table 4. Diamond to graphite transition.

R_F(Å)	B_F(Å)	B_M(Å)	θ_F(°)	θ_M(°)	E_F(eV/atom)	E_M(eV/atom)	p_M
1.54	1.540	1.541	109.5	109.5	0.00	0.024	0.00
1.80	1.510	1.520	106.4	107.9	0.20	0.235	0.32
2.00	1.475	1.489	102.9	105.2	0.33	0.351	0.48
2.20	1.438	1.468	98.5	102.7	0.31	0.296	0.62
2.45	1.424	1.450	94.6	100.4	0.17	0.210	0.75
2.60	1.422	1.441	92.8	99.0	0.10	0.127	0.87
2.90	1.420	1.428	90.5	96.5	0.03	0.017	1.00
3.35	1.420	1.420	90.0	89.9	0.01	0.000	1.00

The columns with the subscript M refer to this work, F to the work of Fahy *et al* (extracted from the graphs in their paper) and energies are referred to hexagonal AB graphite. It should be noted that rhombohedral graphite and diamond are practically degenerate in the *ab initio* calculations, while there is a 24 meV/atom difference in cohesive energy that is correctly given by the proximity cell potential. Given this 24 meV difference, the agreement between this potential and the *ab initio* calculations is very good.

The relaxations were performed using numerical differentiation to obtain the forces and diagonal second-derivatives of energy for each atom. For each Cartesian direction this required three energy evaluations for the atom and its environment of about 30 atoms, but a realistic approximation was to maintain the topology (i.e. the vertex and edge relationships) of the proximity cells and only recalculate the bonding parameters. Given the anisotropy in the graphite structure a crude variable metric approach was used to structural optimization, searching for a minimum of energy along the vector **u**, where:

$$u_{i\alpha} = -(\mathrm{d}E/\mathrm{d}r_{i\alpha})|\mathrm{d}^2E/\mathrm{d}r_{i\alpha}^2|^{-1}$$

for Cartesian coordinate α and atom i, using Brent's method (Press *et al* 1986).

In summary, the proximity-cell potential gives a reasonable account of defect and elastic properties in diamond and graphite and it should yield valuable information about structures that are between the two.

5. The single interstitial in graphite

A proper treatment of the single self-interstitial in graphite has long been a challenge, because its investigation requires long-range lattice relaxation (because of the flexible nature of the sp^2 bonded sheets) and good account of both sp^2 and sp^3 hybridizations. Early attempts have allowed:

(i) rigid layers, small molecules and CNDO calculations (Abrahamson and Maclagan 1984) giving a migration energy of 10 eV!

(ii) flexible layers, but no interstitial-layer binding in a classical potential (Taji *et al* 1986) giving a formation energy of 1.28 eV or with weak binding (Enriquez *et al* 1975) giving 2.5 eV!

(iii) small supercell (18 atoms) of rhombohedral graphite with *ab initio* total energy estimation on in-plane defects allowing only in-plane movements (Kaxiras and Pandey 1988) giving a formation energy of 19.5 eV!

Experiment gives an interlayer interstitial formation energy in the region of 7 eV and a migration energy below 1 eV (Thrower and Mayer 1978). The proximity-cell potential gives formation energies between 6.8 eV and 8 eV, depending on environment, with a structure close to that proposed by Wallace (1966) having the lowest energy (figure 3). In this structure the interstitial occupies a site between two atoms that are stacked one above the other in the c direction. There is a long bond (1.62 Å) from the interstitial to each of these atoms, which have a |p| value of 0.33 and are forced into a near tetrahedral configuration. It is the combination of long bonds and tetrahedral neighbours that forces the layers apart, allowing the single self-interstitial to cause c axis expansion. This is in contradiction to the common assertion that only clusters of

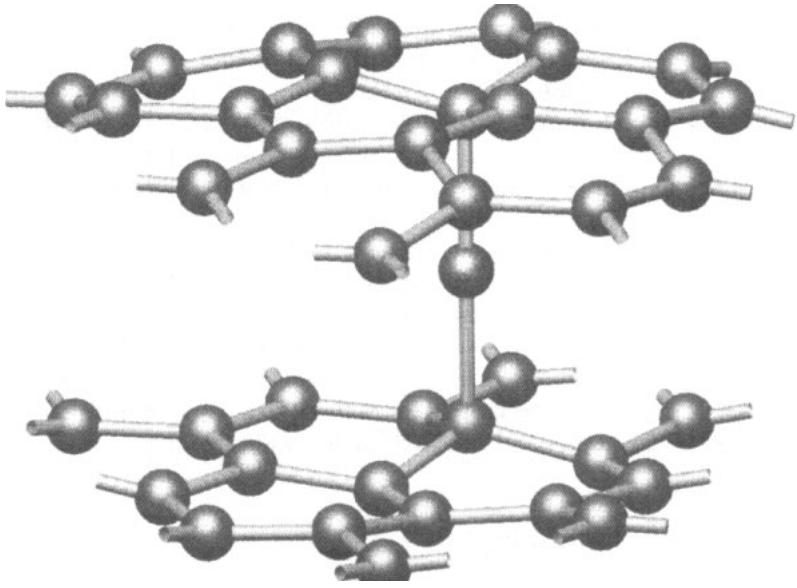

Figure 3. Lowest energy self-interstitial in graphite.

two or more interstitial atoms can cause expansion, because two single C–C bonds of 1.54 Å could not span the 3.35 Å interlayer spacing.

The next-lowest energy position is directly above an atom in one layer and below a hexagonal ring in the next layer. The energy difference between this position and the lowest energy one is between 0.3 eV and 1.3 eV depending on cluster size or unit-cell size. Thrower and Mayer (1978) and Abrahamson and Maclagan (1984) argued that this structure would be the lowest in energy because the interstitial could form four nearly diamond-like bonds with the atom below and three atoms in the hexagonal ring above. The proximity-cell potential makes the three latter bonds unfavourable and prefers to leave atoms in the hexagonal ring perfectly sp^2 hybridized, maintaining the in-plane sp^2 σ- and π-bonds and keeping them orthogonal to the interstitial atomic orbitals.

Two approaches were used in simulating the self-interstitial: supercell and cluster. The supercell was 3x3 unit cells in the basal plane by 2 unit cells in the c direction, giving 72 atoms, with an interstitial atom placed between the middle two layers. All atomic degrees of freedom were relaxed and a formation energy of 6.8 eV was obtained with an expansion of 1.6 atomic volumes in the supercell. The next minimum-energy structure corresponded to a formation energy of 7.1 eV and an expansion of 5.2 atomic volumes. Experimental estimates for the volume of formation vary from 0.9 to 4 atomic volumes (Simmons 1965, Henson and Reynolds 1965) while the modelling of Enriquez *et al* (1975) with very little interlayer binding, gave 6–10 atomic volumes.

The cluster used contained 1945 atoms, with the inner 180 atoms in a near spherical region around the interstitial being relaxed. The lowest formation energy was 6.9 eV and the next lowest 8.2 eV; the greater difference here, compared with the supercell, probably arises from the large formation volume differences and the constant-volume boundary conditions. The superlattice of interstitials is thus a marginally stable arrangement and may be long-lived, possibly giving support to the suggestion by Lachter and Bragg (1986) that it is varying densities of interstitials that give rise to step-like

variations in the value of |c| in graphites of different degrees of perfection. Other, possibly more stable, superlattices are being investigated.

6. Conclusions

The prospect of a reasonable interatomic potential for carbon has come into view with the proximity-cell potential presented here. The potential behaves well for most defects examined and gives useful information about the self-interstitial in graphite by combining good elastic properties with good defect properties. The self-interstitial in graphite is shown to have a ground state structure equivalent to the bonded interstitial first proposed by Wallace (1966) and it has a large formation volume (greater than one atomic volume).

It should be noted that a recent development in the Tersoff potential has been its adaptation to hydrocarbons, including π delocalization energy in a crude way (Brenner 1990). It is anticipated that similar modifications can be applied to the proximity-cell potential in the near future and that sp hybridization can also be included.

Acknowledgments

I would like to thank Professor D J Bacon, Mr C S G Cousins, Dr R Jones, Mr B T Kelly, Mr N McLachlan, Dr P Tole and Dr M O Tucker for helpful discussions. This work was supported by the Central Electricity Generating Board (now Nuclear Electric) and the United Kingdom Atomic Energy Authority. I am grateful to the Computational Science Initiative of the Science and Engineering Research Council (grant GR/F 44977) and the University of Exeter Research Fund who provided the computing facilities.

Appendix A

This appendix describes how the geometrical parameters are obtained for each face, *ij*, representing a bond from atom *i* to atom *j*, in the proximity cell around atom *i*. The parameters are labelled $r_{\sigma_{ij}}$, $\Delta_{1_{ij}}$ and $\Delta_{2_{ij}}$, but in the following the subscript *ij* labelling the face will be dropped for clarity.

The parameter r_σ is based on the maximum inscribed circle, centred on the internuclear intercept, whose radius would be defined as $b_m = \min(b_k)$, where b_k are the perpendicular distances of the edges, k, of length a_k to the internuclear intercept, o (figure A1).

When several b_k are close to b_m, the behaviour of the potential could become chaotic if $r_\sigma = b_m$ were used, so a weighted combination of b_k's is used as below:

$$\omega_k = a_k \exp[-\alpha(b_k - b_m)^2]/[1 + \epsilon/a_k^2]$$

$$r_\sigma = \left(\sum_k \omega_k\right)\left(\sum_k \omega_k/b_k\right)^{-1}$$

with $\alpha = 100\text{Å}^{-2}$ and $\epsilon = 10^{-6}\text{Å}^2$. The term ϵ/a_k^2 with a low value of ϵ suppresses contributions from very short edges and the high value of α allows only those edges

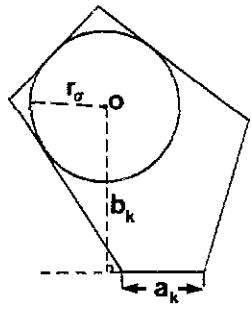

Figure A1. Face parameters for r_σ.

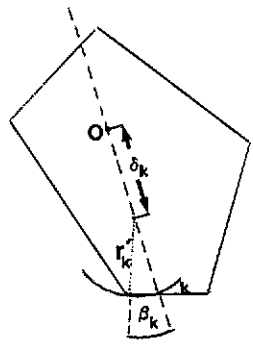

Figure A2. Face parameters for Δ_1 and Δ_2.

with b_k very close to b_m to be significant. The weighted combination represents a softening of the original idea that r_σ could be taken to be b_m, a situation that is recovered if α is made infinite.

The face elongation is probed with circles of variable radius r'_k tangent to the edges,k (figure A2). Letting β_k be the angle between the edge, k, and the projection of $\mathbf{p}_i$ onto the face, then:

$$r'_k = \tfrac{1}{2} r_\sigma [3 - 2\max(\cos\beta_k, \tfrac{1}{2})].$$

The measure of elongation for the edge k is δ_k and is defined in the following way: with the centre of the tangent circle on the line that is the projection of $\mathbf{p}_i$ onto the face, δ_k is the distance from the centre of the circle to the internuclear intercept. The two elongation parameters for the face are then defined as

$$\Delta_1 = r_\sigma + \max(\delta_k) \qquad \Delta_2 = r_\sigma + \min(\delta_k).$$

This procedure gives three well-defined and well-behaved geometrical parameters r_σ, Δ_1 and Δ_2 for each face.

References

Abrahamson J and Maclagan R G A R 1984 *Carbon* **22** 291–5

Bernholc J, Antonelli A, Del Sole T M, Bar-Yam Y and Pantelides S T 1988 *Phys. Rev. Lett.* **61** 2689–92

Biswas R and Hamann D 1985 *Phys. Rev. Lett.* **55** 2001

—— 1987 *Phys. Rev.* B **36** 6434
Biswas R, Martin R M, Needs R J and Nielsen O H 1984 *Phys. Rev.* B **30** 3210–313
Brenner D W 1989 *Phys. Rev. Lett.* **63** 1022
—— 1990 *Phys. Rev.* B **42** 9458–71
Chadi D J 1984 *Phys. Rev.* B **29** 2074
Cousins C S G, 1982 *J. Phys. C: Solid State Phys.* **15** 1857–72
Cousins C S G, Gerward L, Staun-Olsen J and Sheldon B J 1989 *J. Phys.: Condens. Matter* **1** 4511–8
Enriquez F, Quintas M A G and Santos E 1975 *Carbon* **13** 225–31
Fahy S, Louie S G and Cohen M L 1986 *Phys. Rev.* B **34** 1191–9
—— 1987 *Phys. Rev.* B **35** 7623–6
Harrison W A 1986 *Phys. Rev.* B **34** 2787–93
Heggie M I 1989 *Atomistic Simulation of Materials: Beyond Pair Potentials* ed V Vitek and D J Srolovitz (New York: Plenum) pp 347–52
Heggie M I, Jones R and Umerski A **1991** *Phil. Mag.* A **63** 571–85
Henson R and Reynolds R W 1965 *Carbon* **3** 277
Hunter C A and Sanders J K M 1990 *J. Am. Chem. Soc.* **112** 5525–34
Jansen H J F and Freeman A J 1987 *Phys. Rev.* B **35** 8207–14
Kaxiras E and Pandey K C 1988 *Phys. Rev. Lett.* **61** 2693–6
Keating P N 1966 *Phys. Rev.* **145** 637
Kelly B T 1981 *Physics of Graphite* (London: Applied Science)
Lachter J and Bragg R H 1986 *Phys. Rev.* B **33** 8903–5
McSkimin H J and Bond W L 1957 *Phys. Rev.* **105** 116
Nicholson A P P and Bacon D J 1977 *J. Phys. C: Solid State Phys.* **10** 2295–305
Oh D J and Johnson R A 1989 *Proc. MRS Fall meeting (Boston, 1988)* (Pittsburgh, PA: MRS)
Pandey K C 1986 *Phys. Rev. Lett.* **57** 2287–90
Paxton A T and Sutton A P 1989 *Acta Metall.* **37** 1693
Press W H, Flannery P, Teukolsky S A and Vetterling W T 1986 *Numerical Recipes* (Cambridge: University Press) 284
Simmons J H W 1965 *Radiation Damage in Graphite* (Oxford: Pergamon)
Srivastava G P and Weaire D 1987 *Adv. Phys.* **36** 463–17
Stillinger F H and Weber T A 1985 *Phys. Rev.* B **31** 5262–71
Taji Y, Yokota T and Iwata T 1986 *J. Phys. Soc. Japan* **55** 2676–86
Tersoff J 1986 *Phys. Rev. Lett.* **56** 632–5
—— 1988a *Phys. Rev.* B **37** 6991–9
—— 1988b *Phys. Rev.* B **38** 9902–5
Thrower P A and Mayer R M 1978 *Phys. Status Solidi a* **47** 11–37
Wallace P R 1966 *Solid State Commun.* **4** 521
Weinert M, Wimmer E and Freeman A J 1982 *Phys. Rev.* B **26** 4571–8
Yin M T and Cohen M L 1984 *Phys. Rev.* B **29** 6996–8
Zhao Y X and Spain I L 1989 *Phys. Rev.* B **40** 993–7